

Effect of LPPS Spray Parameters on the Structure of Ceramic Coatings

J. Disam, K. Luebbers, U. Neudert, and A. Sickinger

The structure of low-pressure plasma sprayed ceramic coatings on a molybdenum substrate depends on the spray parameters. Porosity decreases with decreasing chamber pressure for all mullite and alumina coatings investigated, whereas the number of cracks decreases for the mullite-type coatings and increases for the alumina-type coatings. The structure of the coatings was analyzed by X-ray diffraction and revealed that the phase content was independent of the chamber pressure. The results indicate that the lowest thermal mismatch exists between the mullite/glass coating and the molybdenum substrate.

1. Introduction

REFRACTORY metals, especially molybdenum, are often used as construction and aggregate material for glass-producing facilities. The limitation of refractory metals is their high oxidation rates above 600 °C. Therefore, the development of high-temperature resistant and gas-tight coatings for refractory metals is an important task. A previous investigation of Henne and Weber^[1] has shown that mullite can be a promising solution for molybdenum because the coefficients of thermal expansion (CTEs) are nearly equal over a wide temperature range (CTE of Mo = $5.8 \times 10^{-6} \text{ K}^{-1}$ and CTE of mullite = $5.6 \times 10^{-6} \text{ K}^{-1}$) and the high-temperature resistance of mullite is sufficient. Examining the influence of chamber atmosphere and pressure^[2] on the structure of low-pressure plasma sprayed (LPPS) mullite coatings revealed that, in the range between 150 and 800 hPa, porosity decreases with decreasing chamber pressure. The best coatings were obtained in an argon atmosphere rather than in air or CO₂.

Coating properties depend on their composition, phase changes that may occur during plasma spraying, coating defect structure, and coating bond. Moreover, the CTEs of coating and substrate are important, since they may result in crack initiation and propagation. The stress in front of the crack tip is influenced by inclusions, grain boundaries, and inhomogeneities (pores, microcracks) affecting energy-absorbing processes such as crack formation, crack branching, and crack growth. Quasi-ductile behavior, i.e., subcritical crack propagation, can be attained by different toughening mechanisms such as fiber reinforcement, transformation toughening, and devitrification. For these reasons, mullite, mullite/glass, mullite/ZrO₂-Y₂O₃, Al₂O₃-MgO, and Al₂O₃-MgO/ZrO₂-CaO were chosen to investigate the influence of some parameters of the LPPS method on the coating structure.

Key Words: alumina, LPPS process, molybdenum substrate, mullite, optimization, porosity, thermal expansion

J. Disam, K. Luebbers, and U. Neudert, Schott Glaswerke, Hattenbergstrasse 10, 55122 Mainz, Germany; and A. Sickinger, Electro-Plasma Inc., 17426 Daimler Street, Irvine, CA 92714.

2. Materials and Processing

The spray powders used are agglomerated and sintered products that consist of a spherical morphology with some satellites (Fig. 1a). At higher magnifications, the singular particles of mullite and mullite/ZrO₂-Y₂O₃ are very sharp edged (Fig. 1b), whereas the single particles of the mullite/glass (Fig. 1c), the Al₂O₃-MgO, and the Al₂O₃-MgO/ZrO₂-CaO powders are much smoother (Fig. 1d). Moreover, many spherical agglomerates are hollow. The grain size distribution was 10 to 45 μm and, therefore, most of the particles are fully molten, partially molten, or in a dough-like plastic state when they impinge on the substrate surface.

The compositions of the powders are shown in Table 1. For the mullite/glass powder, a standard technical glass was used having a transformation temperature (T_g) of 590 °C, a working temperature of 1133 °C, and a CTE of $6.6 \times 10^{-6} \text{ K}^{-1}$. Molybdenum sheets of 50 × 50 × 2 mm having a chemical purity of 99.95% were used as a substrate.

The chamber pressure was varied between 53 and 133 hPa (40 and 100 torr) and the coating thickness between 200 μm and 950 μm. The arc current was 1250 A or 1400 A, respectively. The constant process parameters are shown in Table 2. Note that the spray distance depends on the chamber pressure.

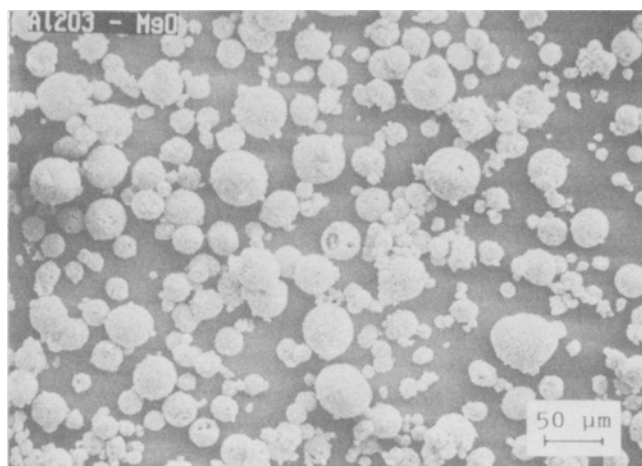
Examination of the coating structure, including porosity and number of cracks, was performed by optical microscopy, scanning electron microscopy, and image analysis. X-ray diffraction was used to characterize phases and reaction products.

Oxidation tests were performed with cylindrical specimens under atmospheric conditions. The specimens had a diameter of 30 mm and a length of 100 mm. The top was rounded to avoid edge cracking, and the heating rate was 50 °C per hour. The test temperature was varied between 1000 °C and 1450 °C, and the testing time was 24 h. All coatings were sprayed at a chamber pressure of 53 hPa with an arc current of 1250 A and 1450 A.

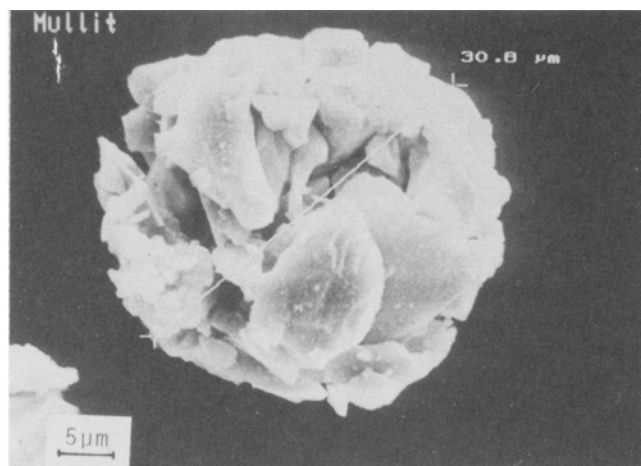
3. Results

3.1 Coating Morphology and Structure

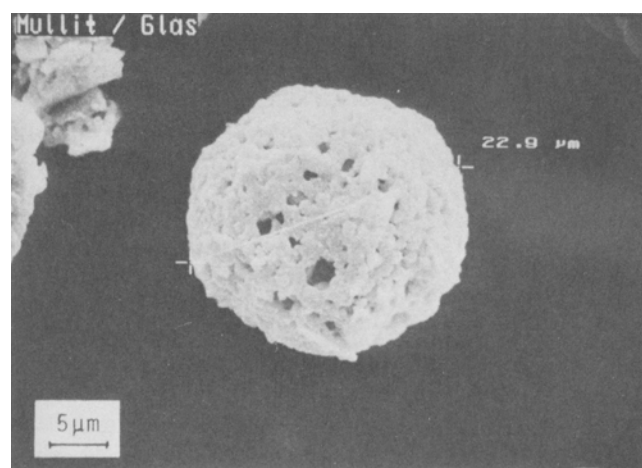
The main requirement for ceramic coatings on refractory metals for high-temperature applications is gas-tightness. The coating porosity and the number of cracks are pertinent criteria. Some pores are needed to compensate for the thermally induced



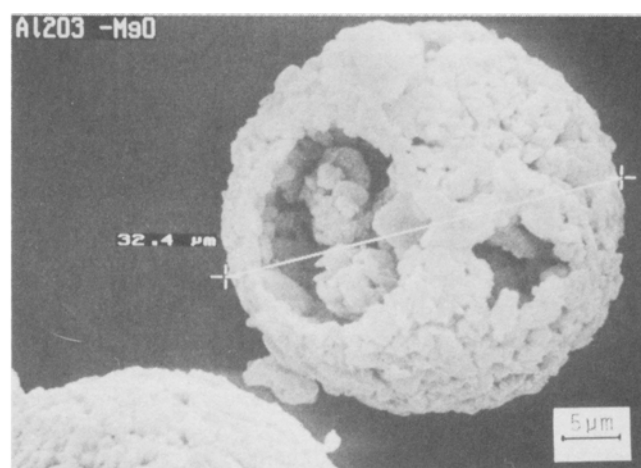
(a)



(b)



(c)



(d)

Fig. 1 Typical morphology of ceramic powders used: (a) spherical agglomerates partially with satellites, (b) mullite and mullite/ ZrO_2 - Y_2O_3 , (c) mullite/glass, and (d) Al_2O_3 -MgO and Al_2O_3 -MgO/ ZrO_2 -CaO.

Table 1 Chemical composition of the powders

Powder type	Composition, wt%
Mullite	28.6% SiO_2 , balance Al_2O_3
Mullite/glass	40.5% SiO_2 , 50% Al_2O_3 , 1-2% B_2O_3 , 5.5% ZnO , 6.5% K_2O
Mullite/ ZrO_2 - Y_2O_3	26.7% ZrO_2 , 2.3% Y_2O_3 , 19.6% SiO_2 , balance Al_2O_3
Al_2O_3 -MgO	27.1% MgO, balance Al_2O_3
Al_2O_3 -MgO/ ZrO_2 -CaO	48.3% ZrO_2 , 3.1% CaO, 13.6% MgO, balance Al_2O_3

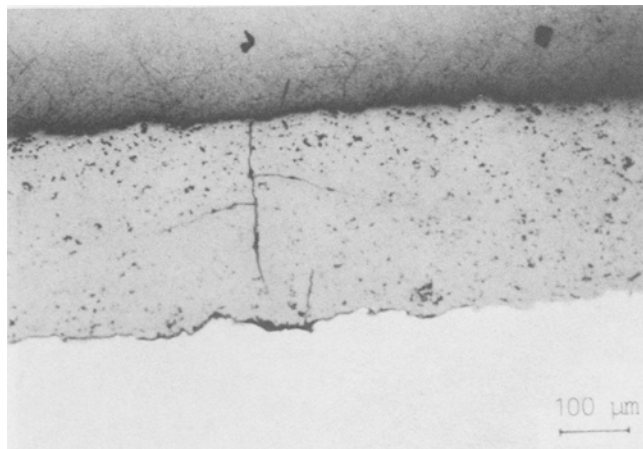
stresses; however, too many pores can lead to open porosity. A great number of cracks indicates the presence of high residual stresses in the coating or between the substrate and coating.

The comparison of the coatings sprayed at an arc current of 1250 A and at a chamber pressure of 80 hPa reveals differences between the five coatings. Mullite and mullite/ ZrO_2 - Y_2O_3 coatings have the highest density. No pore agglomerations can be

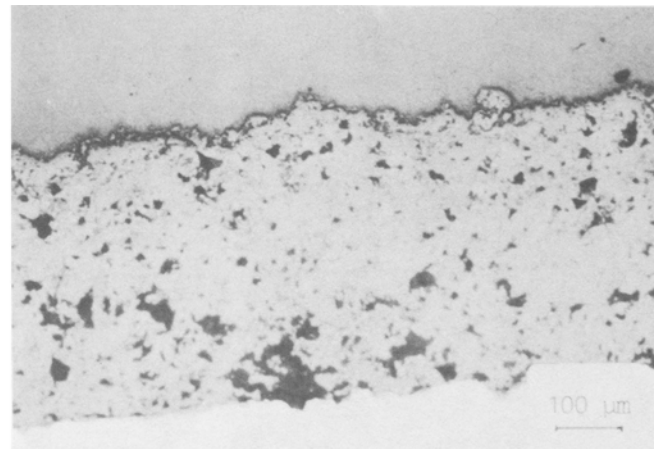
Table 2 Plasma spraying parameters

Plasma spray gun	EPI 03CA-175
Nozzle bore, mm	9.5 diameter
Plasma	Ar: H_2 = 8:1
Arc voltage, V	60
Arc current, A	1250/1400
Powder port, mm	0.43 diameter
Powder feed rate, g/min	30
Carrier gas, psi	40
Spray distance, mm	200 to 330

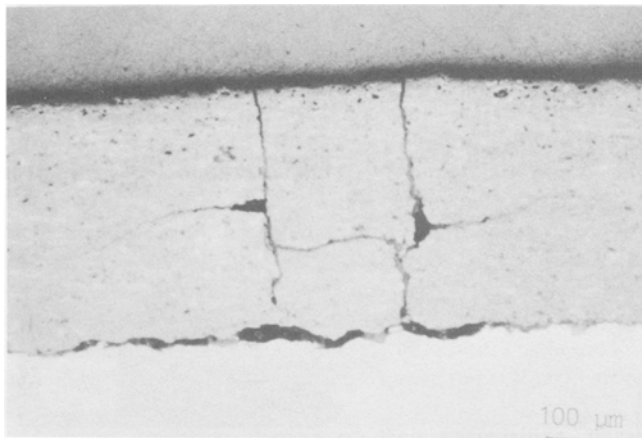
observed, but wide cracks run vertically through the coatings with some branches in the horizontal direction (Fig. 2a, b). The mullite/ ZrO_2 - Y_2O_3 coating also exhibits cracking at the interface between the substrate and the coating. The mullite/glass coatings are much more porous with many pore agglomerations, but at these spraying conditions, no cracking occurs. At chamber pressures above 80 hPa, cracks are present, but they are very



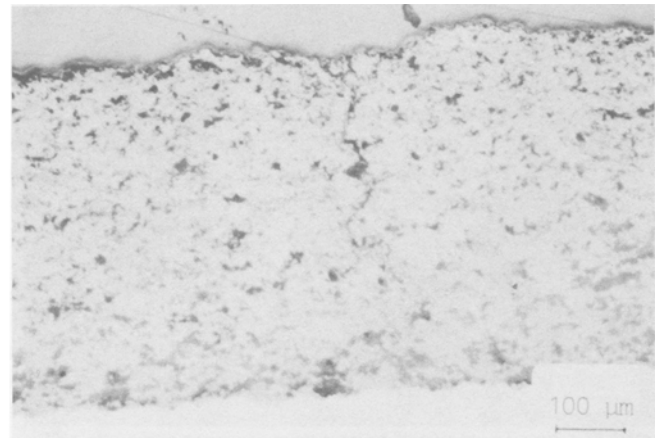
(a)



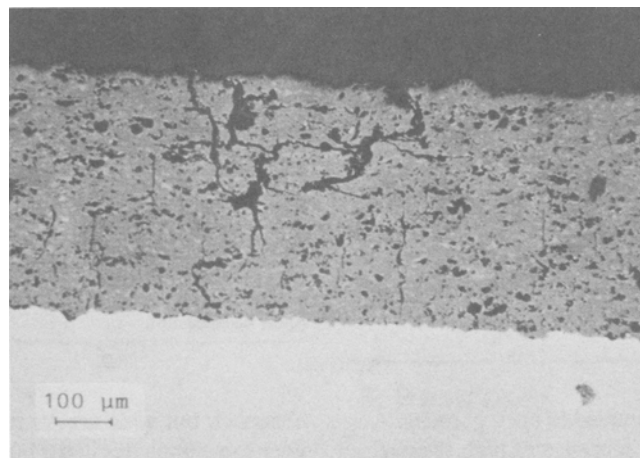
(b)



(c)



(d)



(e)

Fig. 2 Typical morphology of the investigated coatings (metallographic cross sections): (a) mullite, (b) mullite/ ZrO_2 - Y_2O_3 , (c) mullite/glass, (d) Al_2O_3 - MgO , and (e) Al_2O_3 - MgO / ZrO_2 - CaO .

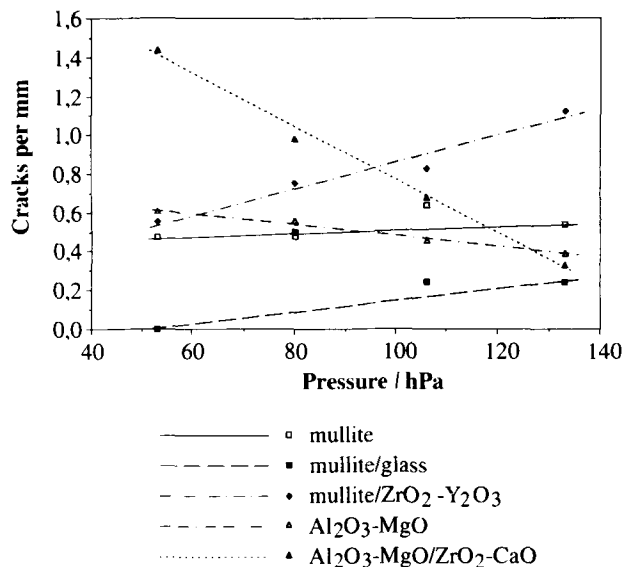


Fig. 3 Influence of chamber pressure on crack formation; arc current: 1400 A, coating thickness: 500 μm .

small and not branched (Fig. 2c). The $\text{Al}_2\text{O}_3\text{-MgO}$ coatings are very porous with irregular-size pores and a great number of unbranched cracks (Fig. 2d). The coating also shows a higher density compared to that of the $\text{Al}_2\text{O}_3\text{-MgO/ZrO}_2\text{-CaO}$ coating. It is significant that a crack network forms at all spraying conditions (Fig. 2e).

The pure mullite coatings exhibited $\text{Al}_6\text{Si}_2\text{O}_{13}$ as the main crystalline component and alumina as a secondary phase. A high portion of the mullite was amorphous as expected from the rapid cooling that took place. In mullite/glass material, no second phase of alumina could be found. The mullite is partially amorphous, and the glass exists in the amorphous phase only. The mullite/ $\text{ZrO}_2\text{-Y}_2\text{O}_3$ material, on the other hand, was fully crystalline. The two mineral phases, $92\text{ZrO}_2\cdot 8\text{Y}_2\text{O}_3$ and $\text{Al}_6\text{Si}_2\text{O}_{13}$, coexist. The predominant part of $\text{Al}_2\text{O}_3\text{-MgO}$ is crystalline and has the composition of MgAl_2O_4 . This mineral phase has a spinel structure, but the amorphous portion is not significant. The structure of $\text{Al}_2\text{O}_3\text{-MgO/ZrO}_2\text{-CaO}$ was also fully crystalline, and in this case, three mineral phases, MgAl_2O_4 , $\text{Ca}_{0.15}\text{Zr}_{0.85}\text{O}_{1.85}$, and ZrO_2 , were present. This indicates that zirconia stabilizes crystallization. The composition and portion of the crystalline phases of the five coatings are not influenced by either chamber pressure or arc current.

3.2 Cracking Behavior

Cracks that pass through the coating thickness to the molybdenum substrate are detrimental to the oxidation resistance. These cracks were counted for all coatings by utilizing metallographic cross sections. The examined length of the specimen was 50 mm, and coating thickness was 300 to 400 μm . The graph of the number of cracks vs. chamber pressure (Fig. 3) reveals that the influence of chamber pressure depends on the coating type. The crack number for the three mullite materials increases with increasing chamber pressure and in the sequence mullite/glass, mullite, and mullite/ $\text{ZrO}_2\text{-Y}_2\text{O}_3$. There is only a small influence of chamber pressure for pure mullite, as indi-

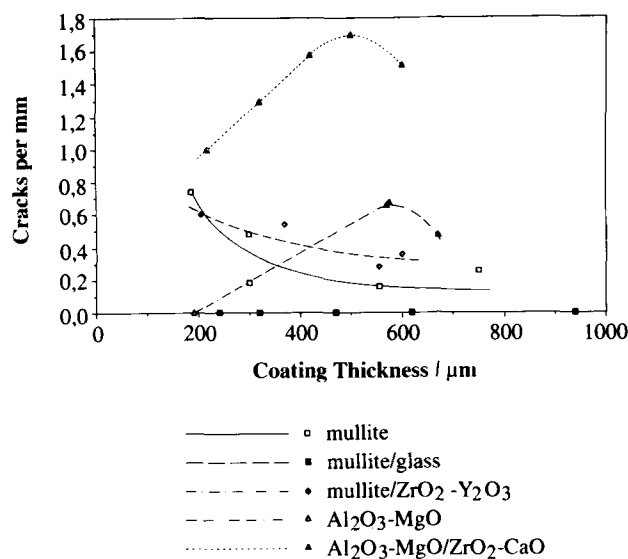


Fig. 4 Influence of coating thickness on number of cracks; arc current: 1250 A, chamber pressure: 53 hPa.

cated by a slow rise of crack number. Note that below chamber pressures of 80 hPa, no cracks are present in the mullite/glass coatings. On the other hand, due to the greater difference between the CTEs, cracking is more pronounced in the mullite/ $\text{ZrO}_2\text{-Y}_2\text{O}_3$ coatings. This is an opposite behavior to that for the spinel-type coatings, where the crack number decreases with increasing chamber pressure. In the zirconia-containing alumina coatings, the highest number of cracks are present. No influence of the arc current on the cracking behavior could be observed.

The influence of coating thickness on the number of cracks was investigated at a chamber pressure of 53 hPa and an arc current of 1250 A (Fig. 4). In the case of mullite/glass, no cracks have been generated at these conditions for any coating thickness. The crack number decreases with increasing coating thickness for mullite and mullite/ $\text{ZrO}_2\text{-Y}_2\text{O}_3$, but the effect is not very distinct. The $\text{Al}_2\text{O}_3\text{-MgO}$ and $\text{Al}_2\text{O}_3\text{-MgO/ZrO}_2\text{-CaO}$ coatings exhibit opposite behavior, where the crack number rises with coating thickness (Fig. 4) due to the formation of a crack network. Above a coating thickness of 600 μm , the crack number decreases slightly because fewer cracks pass through the whole coating. The comparison between the two spinel coatings shows that the addition of 50% $\text{ZrO}_2\text{-CaO}$ leads to more pronounced cracking due to the greater thermal expansion mismatch.

3.3 Porosity

Crack formation and porosity play important roles with regard to oxidation resistance. Open porosity leads to coating failure. Porosity was examined by image analysis using optical and scanning electron microscopy. Figure 5 reveals that, for all coatings, porosity increases marginally with increasing chamber pressure. In mullite it varies between 2.2% at 53 hPa and 3.4% at 133 hPa. Mullite/ $\text{ZrO}_2\text{-Y}_2\text{O}_3$ shows the highest density. Porosity is about 1% lower than that of pure mullite, but the increase with chamber pressure is nearly the same. The 10.5% porosity of

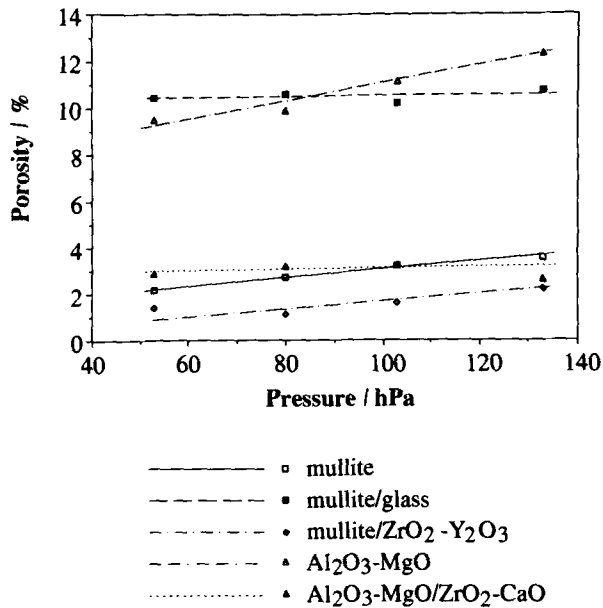


Fig. 5 Influence of chamber pressure on porosity of ceramic coatings; arc current: 1250 A.

Table 3 Oxidation test

Coating	Arc current, A	Test temperature, °C	Failure temperature, °C
Mullite	1400	1000	n.f.
Mullite	1400	1450	800
Mullite	1400	1450	960
Mullite	1400	1450	1195
Mullite	1250	1450	1000
Mullite/glass	1400	1000	n.f.
Mullite/glass	1400	1450	1160
Mullite/glass	1400	1450	1185
Mullite/glass	1400	1450	1375
Mullite/glass	1250	1450	n.f.

n.f. represents no failure.

the mullite/glass coating is about three times higher than the pure mullite. Some of the glass volatilizes during spraying due to its lower thermal stability; therefore the porosity is high and the influence of chamber pressure becomes negligible. The porosity of the pure Al₂O₃-MgO varies between 9.5% at 53 hPa and 12% at 133 hPa, whereas the porosity of Al₂O₃-MgO/ZrO₂-CaO is in the same range as mullite (about 3%). The addition of zirconia increases the density of mullite and spinel coatings by lowering the porosity.

3.4 Oxidation Resistance

An oxidation test was used to determine the functionality of the coatings. If open porosity is present or if cracks penetrate through the coating to the molybdenum substrate, then rapid oxidation takes place, and MoO₃ vapor can be observed above 600 °C. The test involved heating the coating to the temperatures of 1000 °C and 1450 °C. The temperature at which the MoO₃ vapor was detected was recorded as the failure temperature. The results for mullite and mullite/glass coatings are given in Table 3.

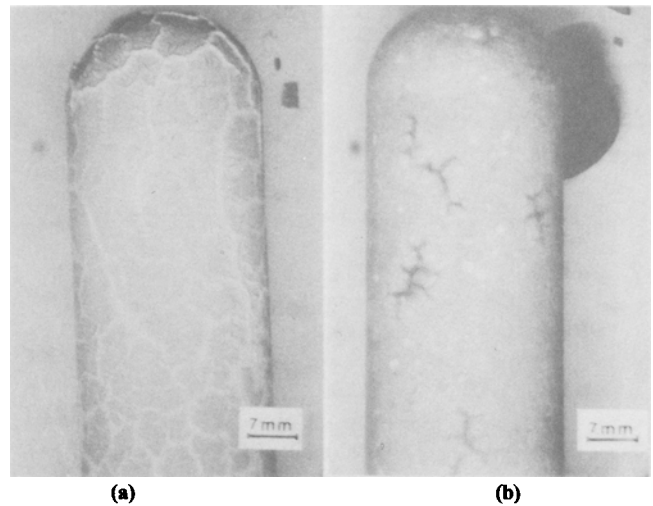



Fig. 6 Coating morphology after the oxidation test; arc current: 1250 A, chamber pressure: 53 hPa, heating rate: 50 °C/h; (a) mullite coating, failed at 1000 °C, and (b) mullite/glass coating after 24 h at 1450 °C.

At the test temperature of 1000 °C, both coatings achieved the limit of the 24 h test time. On the other hand in some tests, the mullite coating failed at temperatures below 1000 °C. No mullite coating reached 1450 °C. The mullite/glass material exhibited a higher temperature resistance than pure mullite since this coating did not fail below 1160 °C. The mullite/glass coating, sprayed at an arc current of 1250 A, attained an end-of-test time at 1450 °C. Figure 6 shows the photograph of a mullite coating that failed at 1000 °C during heating (Fig. 6a) and of a mullite/glass coating after 24 h at 1450 °C (Fig. 6b). In the case of mullite, many cracks have been generated, whereas in mullite/glass no cracks are present. The cracks shown in this photograph are generated during cooling.

4. Discussion

Plasma spraying in a controlled low-pressure environment results in the improvement of coating qualities due to the elimination of oxygen entrainment and oxide inclusions. Although at low pressures the plasma heat transfer is not very efficient, the LPPS process melts most powders over a larger jet diameter and length than in atmospheric spraying. Higher jet exit velocities are also obtained. LPPS has also lowered the turbulent gas entrainment and plasma jet temperature. Therefore, the traversing particles are more uniformly treated, which leads to high density and good bond between the substrate and coating.^[3,4] Examination of the coating structures reveals that the effect of the spray parameters investigated depends on the coating type.

Porosity decreases with decreasing chamber pressure for all coatings, since the higher particle velocity at low chamber pressures leads to good contact and adhesion between the particles and a high density.^[4] The particle velocity decreases, i.e., the dwell time rises with increasing chamber pressure, and therefore more particles are fully molten. This leads to the formation of voids within the coating.^[5] The lower density of the Al₂O₃-MgO coating compared to the mullite coating is due to



the higher melting temperature of alumina. In the case of mullite/glass, the high porosity is most likely caused by the lower thermal stability of the glass, i.e., most of the particles are liquid and may partly vaporize during spraying. Therefore, many pores are formed within the coating.

The addition of stabilized zirconia leads to a more dense two-phase structure of the coating but also to a higher crack number due to the greater thermal expansion mismatch. Cracking behavior is different for the mullite- and spinel-type coatings. The crack number decreases with decreasing chamber pressure for the mullite-type coatings whereas it increases for the spinel coatings. For pure mullite, there is only a slight influence of chamber pressure on crack number. This may be an effect of the highly amorphous portion, which leads to lower brittleness and some self-healing capability.^[1] Cracking behavior is improved by the addition of glass due to the higher amorphous phase content. On the other hand, cracking is more pronounced in the zirconia-containing coatings because of the greater difference of the CTEs and the fully crystalline structure. In the case of the spinel-type coatings, the decrease of crack number with increasing chamber pressure is due to the increase of jet temperature and dwell time. Therefore, less cracks are formed; this results in better adhesion between the single particles and a higher strength coating. Any pores that are present may stop crack growth.

The slight increase of crack number with increasing coating thickness for the mullite-type coatings is an effect of heat transfer of both the coating and substrate. At low coating thicknesses, heat transfer is determined by the molybdenum substrate, i.e., more rapid cooling initiates cracking, whereas cooling rates are less at higher thicknesses because of the lower heat conductivity of the coating materials. In the case of the spinel-type coatings, the number of cracks increases with coating thickness and forms a crack network. Above a coating thickness of about 600 μm , less cracks penetrate through the whole coating, leading to a slight decrease of crack number.

The results of the oxidation tests show that the mullite/glass coating may be a promising solution for the intended application. This coating has a certain self-healing capability because the glass is ductile above the critical temperature of 600 $^{\circ}\text{C}$, where rapid MoO_3 formation occurs. All cracks that were present were generated after the oxidation test during cooling.

5. Summary

The investigation of low-pressure plasma sprayed mullite and spinel coatings has demonstrated that the coating composi-

tion is of greater influence than chamber pressures lower than 133 hPa and the change of arc current from 1250 A to 1450 A.

Porosity decreases with decreasing chamber pressure for all coatings due to the higher particle velocity, which leads to better adhesion and a higher density. Crack number rises slightly with chamber pressure for pure mullite, whereas in the zirconia-containing mullite coating, cracking is more pronounced due to the greater thermal expansion mismatch. No cracks are present below chamber pressures of 80 hPa for mullite/glass coatings. On the other hand, the number of cracks that penetrate to the substrate falls with increasing chamber pressure for the $\text{Al}_2\text{O}_3\text{-MgO}$ and $\text{Al}_2\text{O}_3\text{-MgO/ZrO}_2\text{-CaO}$ coatings, and a crack network is formed. The influence of coating thickness on the cracking behavior is an effect of the heat transfer. At lower thicknesses, heat transfer is determined by the molybdenum substrate, whereas at higher thicknesses, the lower heat conductivity of the coating material leads to lower cooling rates. X-ray diffraction analysis showed that the portion of amorphous and crystalline components is independent on chamber pressure but depends on the coating composition.

These results reveal that mullite and mullite/glass materials are potential coatings for refractory metals in high-temperature applications. A mullite/glass material will be the best coating if no open porosity is present. $\text{Al}_2\text{O}_3\text{-MgO}$ and $\text{Al}_2\text{O}_3\text{-MgO/ZrO}_2\text{-CaO}$ coatings are not suitable due to the formation of a crack network.

References

1. R. Henne and W. Weber, Progresses in the Development of High-Temperature, Oxidation Protective Coatings for Molybdenum Utilizing the Low Pressure Plasma Spraying Process (in German), *Proc. Conf. of the 11th Plansee Seminar*, Reutte/Tirol, Austria, 1985, p 189-206
2. J. Disam, A. Sickinger, and V. Wilms, The Effect of the Chamber and Spraying Parameters of the LPPS Method on the Structure of Mullite Coatings, in *Thermal Spray Research and Applications*, T.F. Bernecki, Ed., ASM International, Materials Park, OH, USA, 1991, p 533-538
3. R.W. Smith, Plasma Spray Processing ... The State of Art ... and Future—From a Surface to a Materials Processing Technology, *Proc. Conf. of the 2nd Plasma-Technik-Symposium*, S. Blum-Sandmeier, H. Eschnauer, P. Huber, and A.R. Nicoll, Ed., Luzern, Switzerland, 1991, p 17-38
4. R. Henne and W. Weber, Plasma Spraying at Low Pressure, a Process for Producing Dense Coatings for High Melting Metals (in German), *Proc. Conf. of the 10th Plansee Seminar*, Reutte/Tirol, Austria, 1981, p 283-295
5. H. Liu, E. Mühlberger, A. Sickinger, E. Lavernia, and R.H. Rangel, Deformation and Interaction Behavior of Molten Droplets Impinging on a Flat Substrate in Plasma Spray Process, in *Thermal Spray Coatings: Research, Design and Applications*, C.C. Berndt and T.F. Bernecki, Ed., ASM International, Materials Park, OH, USA, 1993, p 457-462